

# Beyond Accuracy: Statistical Measures and Benchmark for Evaluation of Representation from Self-Supervised Learning

Jiantao Wu<sup>1\*</sup>, Shentong Mo<sup>2</sup>, Sara Atito<sup>1</sup>, Josef Kittler<sup>1</sup>, Zhenhua Feng<sup>1</sup>, Muhammad Awais<sup>1</sup>  
<sup>1</sup> University of Surrey, <sup>2</sup> Carnegie Mellon University

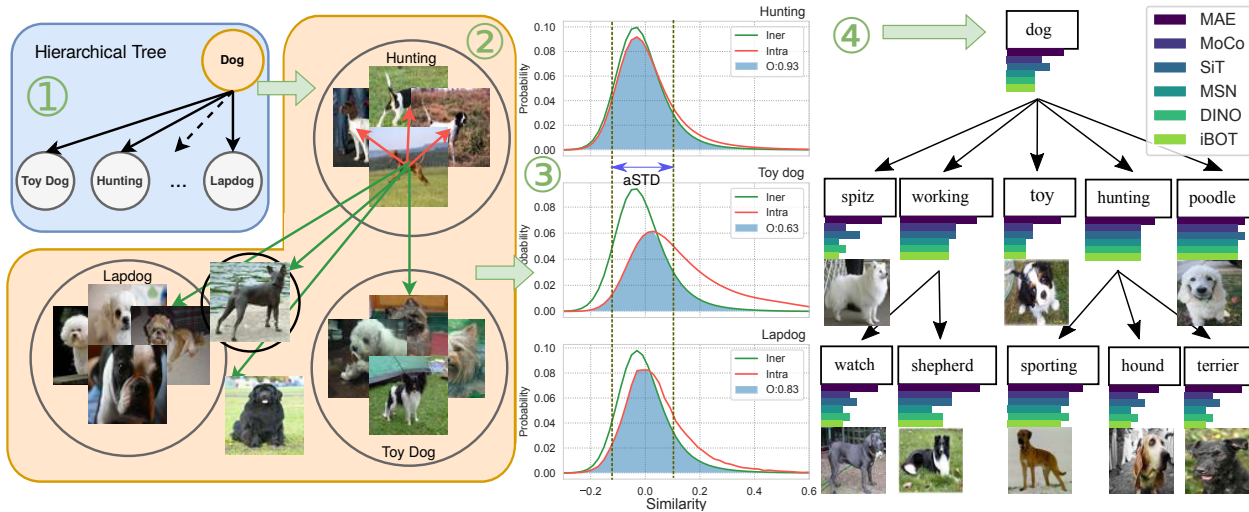


Figure 1. Overview of evaluating synsets in WordNet by these steps: 1) Construct the hierarchical tree for a synset “dog.n.01”, utilizing WordNet. 2) Build clusters for the direct children of the synset. Each cluster contains all samples belonging to the child in ImageNet-21K. 3) Compute both inter- and intra-similarity distributions for each cluster, and calculate the overlap (O) and average standard deviation (aSTD) to elucidate the degree of separability between clusters and the internal consistency of similarity distributions across clusters respectively. 4) Evaluate all synsets for SSL models and compare their overlap. The size of a color bar denotes the value of overlap for its corresponding model in the legend (lower the overlap better it is).

## Abstract

Recently, self-supervised metric learning has raised attention for the potential to learn a generic distance function. It overcomes the limitations of conventional supervised one, e.g., scalability and label biases. Despite progress in this domain, current benchmarks, incorporating a narrow scope of classes, stop the nuanced evaluation of semantic representations. To bridge this gap, we introduce a large-scale benchmark with diversity and granularity of classes, Statistical Metric Learning Benchmark (SMLB) built upon ImageNet-21K and WordNet. SMLB is designed to rigorously evaluate the discriminative discernment and generalizability across more than 14M images, 20K classes, and 16K taxonomic nodes. Alongside, we propose novel evaluation metrics – ‘overlap’ for separability and ‘aSTD’ for consistency – to measure distance statistical information,

which are efficient and robust to the change of class number. Our benchmark offers a novel perspective of evaluating the quality of representations beyond accuracy. Our findings reveal the limitations of supervised learning and the class bias inherent in SSL models, offering insights into potential areas for future model enhancement.

## 1. Introduction

Representation learning in computer vision has gained significant attention in recent years both in terms of supervised representation learning via metric learning [22, 23, 42, 47] and self-supervised representation learning [2, 3, 7, 19, 26, 30, 45, 46]. Metric learning aims to learn an optimal distance metric to measure the similarities of samples [22, 42, 47], where samples from the same class will have small distances while samples from different classes

will be far apart in the learnt embedding space. This capability of representation learning enables various tasks, notably in classification (e.g., facial recognition [25]), clustering (e.g., image clustering [6, 20]), and retrieval (e.g., image retrieval [14]). Typical metric learning methods like contrastive loss [17] and triplet loss [38] require annotated data to form positive and negative pairs or triplets to optimize the distance metric.

However, supervised metric learning methods are designed for measuring the semantic distances in specific domains. For example, ArcFace [11], trained on CASIA-WebFace [48], can only perform well on face-related tasks. In addition, they have limitations on scaling to large datasets [9, 39]. It relies on label information, which can be expensive and time-consuming to obtain. The finite class labels also can not capture the full semantic similarities between samples due to the complexity and uncertainty of real-world problems. In addition, the sampling of pairs or triplets can bias the embedding space because of label imbalance [34]. All these obstruct learning a general distance metric to measure the semantic distance for arbitrary inputs.

Recent self-supervised learning methods address these limitations by pretraining on unlabeled data [2, 3, 5, 7]. They design pretext tasks to learn semantic representations, which allows for learning more meaningful metrics without human annotations. For example, contrastive methods like SimCLR [7] aim to pull together representations for different augmented views of the same image while pushing apart views from different images. Recently, self-supervised methods have shown great promise in learning representations with improved metrics over supervised counterparts [2, 5, 7, 13, 24, 27, 28]. They are more data-efficient and can model fine-grained semantic similarities beyond discrete class labels [2, 4]. Fu et al. [16] proposed a self-supervised ranking framework to capture intra-class characteristics. Despite the use of SSL, it only plays as an auxiliary regularizer and still requires labels to learn discriminative features for inter-class samples. Wang et al. [43] gets rid of labels by contrastive quantization with code memory to learn binary hash codes for a dataset. However, they did not explore contrastive learning as a general distance measurement. A statistical framework of self-supervised metric learning in the context of multi-view data is developed by Wang [44], yet, lacks a reality check for the existing family of SSL methods and on real problems. To bridge the gap, we conduct a large-scale empirical study on the evaluating semantic distinctions of learned representations from diversity and granularities.

The first obstacle is the lack of diversity and granularity of classes in the existing benchmarks. Current benchmarks specialize a narrow scope, such as Oxford and Paris Buildings [33], face identification [23] and Pets [31]. Moreover, the flattened label structure in these benchmarks is infeasible

to reveal granularity of classes. For instance, two dogs of subordinate breeds, e.g., Pekingese and Maltese, should be closer than two arbitrary dogs. Therefore, we do not know the how well the semantic representation is as a general semantic distance function to measure the similarity between two arbitrary images. The second obstacle is the insufficiency of metrics for representations. The popular metrics, e.g., accuracy, cannot provide a complete picture of embedding space [29]. These metrics, losing the distance information, only reveal a final task performance. We consider two desirable properties of representation *separability* and *consistency*, i.e., the degree to which distinct clusters are distinguishable from one another in the feature space, and the uniformity and reliability of similarity distributions across clusters.

To tackle the above problems, we build a novel benchmark, Statistical Metric Learning Benchmark (SMLB), on the top of ImageNet-21K [37] and WordNet [15]. This large-scale benchmark consists of 14,191,291 images divided into 20,498 classes and 16,632 taxonomic nodes. This large-scale benchmark allows a wide examination of the model’s ability to identify and differentiate nuanced distinctions within data, termed *discriminative discernment*, as well as generalizability. We further propose a novel evaluation to measure the distance statistical information from the distributions between inter- and intra- pairs. To depict the characters of similarity distributions, we propose two novel metrics: *overlap* to measure separability and *aSTD* to measure consistency. Figure 1 shows the overview of our work. We create clusters for a synset based on its hierarchical tree and evaluate the corresponding overlap and aSTD. Then, we examine a wide range of SSL models with mono- or hyper-SSL techniques, e.g., view contrast, masked image modeling, and knowledge distillation on SMLB with *overlap* and *aSTD* to conduct an empirical study of learning semantic representations through SSL. Finally, our study leads to important findings. Our contributions can be summarized as:

- We propose two metrics based on statistical information to evaluate the distance functions: *overlap* reveals separability, *aSTD* reveals consistency.
- We build a large-scale Statistical Metric Learning Benchmark, *SMLB*, to make a comprehensive evaluation of discriminative discernment and generalizability.
- From a bunch of experiments, we empirically find 1) the detrimental potential of supervised learning. 2) class bias of self-supervised learning.

## 2. Related Work

**Benchmarks for Metric Learning.** In metric learning, benchmarks are pivotal for evaluating the ability of algorithms to learn distance or representation functions for narrow tasks. For example, WebFace [48] contains 494,414 face images of 10,575 real identities, which is used for

face verification and face identification. Oxford and Paris Buildings [33] are popular for image retrieval, which has 5,062 and 6,412 images from 11 landmarks. These benchmarks lack diversity to assess the representation for a general distance function to measure the semantic distance. Task Adaptation Benchmark (VTAB) [10] is a benchmark with diverse, unseen tasks with few examples for a unified evaluation for general visual representation, yet, not designed for a distance measurement. Though ImageNet-21K (IN21K) [37] was proven suitable for pretraining, there is no study to evaluate models, utilizing its 21K classes with hierarchical semantics from WordNet [15]. In this work, we build a large-scale benchmark based on IN21K and WordNet for metric learning to validate discriminative discernment which refers to the capacity for making or recognizing detailed distinctions of the learned representations of SSL models.

**Performance Measures for Metric Learning.** Accuracy, Precision, Recall, F1-score, Normalized Mutual Information (NMI), and mean average precision (mAP) are popular metrics to report the performance. Musgrave et al. [29] shows the weakness of accuracy metrics and concludes that it cannot provide a complete picture of embedding space, i.e., accuracy fails to show the separation of different classes. In addition, the accuracy loses distance information causing a lack of comprehensive assessment of representations. Some studies highlight the importance of distance-based metrics for the representations. Inter-class Similarity and Intra-class Deviation are two important aspects to promote the quality of representations [41]. Rippel et al. [36] promote separability by penalizing class distribution overlap. In this work, we preserve the distance information by histogramming similarity distributions and propose two metrics overlap and aSTD to evaluate their separability and consistency.

**Evaluation Protocol.** The finetune protocol is one of the most pivotal evaluations for SSL models [12]. Linear prob is another popular evaluation protocol, which does not change the representations and only trains a linear classifier. However, the above two protocols require lots of computational resources to train. What’s worse, they change or re-weight the features to fit new tasks, cannot represent the encoding of meaningful information where the similarity in feature space corresponds to semantic distance. Other prevalent evaluations, e.g., KNN and retrieval, are sensitive to the number of classes. This implies that these evaluations do not adjust or react in proportion to the complexity added by having more classes. For instance, 50% accuracy in a binary classification task is not better than 40% accuracy in a triple classification task. All these motivate us to propose a flexible and unified evaluation protocol to evaluate semantic representations from these considerations.

### 3. Proposed Evaluation Method

#### 3.1. A Distance Perspective

The main goal of this paper is to evaluate the SSL models from the distance perspective. A theoretical analysis is done by Wang [44] where they assume observed data samples, denoted as  $X$ , emanate from a confluence of latent factors and stochastic noise. The latent factor model draw the multi-view data  $(X_1, \dots, X_n)$  as  $X = BZ + e$ , where  $Z$  signifies the latent factors,  $B$  is a transformation matrix such that  $B^T B = \Lambda$ , and  $e$  represents normally distributed noise. However, their analysis is designed for Mahalanobis distance, lacking a reality check for deep neural networks.

To bridge the gap, we introduce an assumption on the modeling of factors for a class modulated by external labels,  $Y$ , that is, the appearance of attribution variable  $Z_i$  is subjected to a Bernoulli distribution such that  $Z_i|Y \sim \text{Bernoulli}(p_i)$ . For instance, the visibility of eyes in a face image could be influenced by whether the person is wearing sunglasses or not. Consequently, the probability of the factor’s (eye’s) presence or absence in the image of a human face.

The distance,  $s(X_1, X_2) = \sum_i Z_1 Z_2$ , is ingeniously crafted as the dot product of the latent factor vectors, signifying the number of shared factors between two samples. Since the presence of each factor is determined probabilistically, the distance metric obeys a Poisson distribution or a normal distribution when there are enough attributions. Therefore, the distance between classes reveals the count of shared attributions. We hypothesize that the distance between samples obeys a normal distribution and the pairs from the same class are significant closer than those from different classes. In the following, we define *intra* pairs as the pairs having the same class, and *inter* pairs as the pairs having different classes. It is notable that the definition is flexible, depending on the content we are studying. The positive pairs can be two images with the same class or two patches of an object from one image. For simplicity, we adopt the former definition by default.

**Similarity Definition.** To compare the global features for images, we define the *intra-class* pair as the pair of images from the same class, and *inter-class* pair as the pair of images from different classes. For a given set of images, denoted as  $\{x^i\}$ , and their corresponding labels  $\{y^i\}$ , we can formulate the intra- and inter-class similarities as follows:

$$\begin{aligned} s_{y^i}^+(\mathbf{x}^i, \mathbf{x}^j) &= \text{sim}(\mathbf{z}^i, \mathbf{z}^j), \text{ if } y^i = y^j, \\ s_{y^i}^-(\mathbf{x}^i, \mathbf{x}^j) &= \text{sim}(\mathbf{z}^i, \mathbf{z}^j), \text{ if } y^i \neq y^j. \end{aligned} \tag{1}$$

To measure the similarity between features, we employ the cosine similarity function, denoted as  $\text{sim}(\cdot, \cdot)$ , which ensures the range of distance from -1 to 1.

**Similarity Distribution.** The similarity distributions describe the likelihood of similarity for the distance of posi-

tive or negative pairs, which provides succinct summaries of distance information beyond accuracy. To calculate the probability density function (PDF) of similarity scores  $s$  in condition, we have

$$p(s|y) = \int_{\mathcal{Z}} \int_{\mathcal{Z}} p(s = \text{sim}(z1, z2)|y) p(z1, z2|y) dz1 dz2 \quad (2)$$

where  $p(z1, z2|y)$  is the joint probability density of the feature vectors given the class label  $y$ ,  $\mathcal{Z}$  is the feature space for positive features or negative features. However, the real similarity distributions  $p(s|y)$  are infeasible. We apply random sampling to get sample pairs and utilize a histogram from -1 to 1 with 100 bins to estimate their distributions. For each class, we can draw inter- or intra- similarity distributions  $p^+(s|y), p^-(s|y)$ . For example, we obtain the distributions by positive pairs for intra-similarity, denoted by red, and negative pairs for inter-similarity, denoted by green, as shown in Figure 1 ②.

### 3.2. Evaluated Models

We address the challenge of learning semantic distance measurement through the self-supervised pretraining of Vision Transformers (ViTs). Our problem setup is described using the following notation: An image, represented by  $\mathbf{x}$ , is divided into non-overlapping patches  $\mathbf{x}_p$ , with  $p$  ranging from 1 to  $N$ , where  $N$  is the total number of patches. A learnable classification (CLS) token, initialized with random weights, is appended to these patches. The ensemble of the CLS token and image patches is then processed by a transformer encoder, denoted as  $f(\cdot)$ , which concurrently extracts local and global features. The CLS token,  $z = f(\mathbf{x})$ , represents the entire image.

In the realm of self-supervised methods, three prominent and fundamental approaches are contrastive learning (CL) [1, 18], masked image modeling (MIM) [3, 19], self-distillation (SD) [5, 50]. For mono-SSL, we examine three representative methods: **MoCov3** [8] advances CL by using a momentum encoder to improve the consistency and quality of visual representations learned from different views of the same image. **MAE** [19] learns rich image representations by MIM to reconstruct the original image content from partially masked inputs. **DINO** [5] employs an SD approach, where a student network learns to predict the output of a momentum teacher network across different augmentations of an image. For hybrid-SSL, we consider three models: **iBOT** [50] extends the SD framework of DINO by applying MIM to patch tokens. **MSN** [1] merges MIM with SD to cultivate detailed and robust representations. **SiT** [2] implements MIM on patch tokens and CL on the CLS token, enhancing the quality of representations in a synergistic manner.

We observe that feature normalization plays a vital role in accurately gauging semantic distances. Consequently, we

standardize the features using the mean and standard deviation derived from the target dataset’s features. For further details, please refer to Section 9.1.

### 3.3. Proposed Metrics

We propose two novel metrics, *overlap* and *average Standard Deviation (aSTD)*, to delve deeper into the nuances of similarity distributions and thereby gain a more insightful understanding of the features. These metrics are applied to a labeled dataset to identify positive and negative pairings. Unlike the conventional metric of *accuracy*, which evaluates the end-to-end performance of a task, our proposed metrics focus on the statistical factors of features, specifically examining *separability* and *consistency*. We illustrate our metrics in Figure 1 ③.

**Overlap.** *Separability* indicates distinctiveness of features, meaning that features from different classes can be delineated by a decision boundary. In our analysis, we aim for the inter-class and intra-class distributions to be sufficiently distinct, allowing for a threshold that separates them. However, finding an optimal, consistent threshold for each class is challenging. As an alternative, we measure *separability* using *overlap*, which is the intersection area between the two distributions. The overlap is calculated using the probability distributions of distances or similarities within the same class (intra-class) and between different classes (inter-class), as shown in the following equation:

$$O = \frac{1}{N} \sum_{y=1}^N \sum_{b \in \mathcal{B}} \min(p^+(s|y \in b), p^-(s|y \in b)), \quad (3)$$

where  $b$  is the bin of similarity range,  $p^+(\cdot), p^-(\cdot)$  denote the probability of the similarity in the bin for positive and negative pairs,  $N$  denotes the number of classes,  $\mathcal{B}$  is the set of bin edges.

The overlap metric ranges from 0 to 1, reflecting the binary classification error when determining if a pair of features belongs to the same class. In an ideal scenario with only two classes, the classification performance is equivalent to finding an optimal similarity threshold for binary classification, with the goal of achieving zero overlap to ensure complete separability of inter-class and intra-class features.

**Average Standard Deviation.** *Consistency* pertains to the stability of the distributions across all classes. We aim for the inter-class and intra-class distributions to maintain a consistent shape for each class. To quantify this, we introduce *aSTD*, the average deviation of distributions across different classes, to capture the deviation within the dataset. This metric is particularly useful for assessing the diversity of a dataset with numerous classes that may vary significantly or be closely related semantically. To calculate *aSTD*, we first determine the conditional similarity distributions  $p(s|y)$  for each class label. We get the distribution

by  $p(s) = \frac{1}{N} \sum_{y=1}^N p(s|y)$ . The average Standard Deviation is measured using the following formula:

$$\begin{aligned} \mu &= \sum_{b \in \mathcal{B}} p(s \in b) \cdot \text{MEAN}(b), \\ \sigma &= \sqrt{\sum_{b \in \mathcal{B}} p(s \in b) \cdot (\text{MEAN}(b) - \mu)^2}, \end{aligned} \quad (4)$$

where MEAN calculate the center of an edge,  $p(s \in b)$  denotes the probability of similarity falls in  $b$ .

aSTD serves as an indicator of the disparity among similarity distributions. A higher aSTD value suggests a greater degree of variance between these distributions, which implies that more effort is required to reconcile these differences. In practice, the aSTD of inter-similarity distributions across classes indicates the potential for performance enhancement through learning processes.

### 3.4. Metric Validation

In this section, we aim to substantiate the reliability and significance of our metrics. To this end, we trained MoCo v3, DINO, and MAE using ViT-S/16 on the IN1K dataset for 300, 200, and 800 epochs, respectively, and saved intermediary weights to obtain 10 checkpoints for each model. These models yield representations of varying quality, providing a broad spectrum of data points to demonstrate the correlation.

To affirm the efficacy of overlap and aSTD, we assessed these models and compared our findings with standard evaluations. We utilized KNN (k=10) and linear probing (over 100 epochs) to measure accuracy on IN1K. Figure 2 illustrates the correlation between our metrics and both the error rate and the performance gap. The data reveal that overlap and inter-class aSTD correlate strongly with the error rate and gap ( $r=0.99, 0.96$ , respectively). In contrast, intra-class aSTD is not as important as inter-one. For convenience, we report aSTD denoting inter aSTD by default. In conclusion, the overlap metric can serve as an indicator of the error rate associated with KNN performance, while aSTD signifies the precision of that indicator.

## 4. Statistical Metric Learning Benchmark

ImageNet-21K (IN21K) [37], a superset of ImageNet-1K, comprises 14,197,087 images divided into 21,841 classes. It is organized according to the WordNet [15], providing hierarchical semantics in multiple levels. We propose a novel benchmark, Statistical Metric Learning Benchmark (SMLB), based on IN21K and our proposed metrics to conduct a thorough evaluation of SSL models in the context of metric learning. This benchmark is meticulously crafted to establish a robust standard for quantifying semantic distance in a large-scale and multiple-grained as well as assessing model generalizability across various contexts.

## 4.1. Benchmark Composition

**Data Curation.** IN21K exhibits a skewed distribution of class representation, with certain classes only containing a minimal number of images, occasionally as low as one. These underrepresented classes fail to offer a dependable intra-class variability. To rectify this, we first selectively curated a subset, hereafter designated as IN20K, which consists of 20,498 classes and 14,191,291 images, by omitting classes comprising less than ten images. Second, we constructed the semantic taxonomy having more than 2 children in accordance with WordNet, where the structure includes 16,632 nodes. Each image is uniformly resized to a resolution of 224x224 pixels and normalized based on the established ImageNet mean and standard deviation parameters.

**Inconsistency.** The inherent complexity of IN21K poses challenges in maintaining accurate image classifications, an issue prevalent in large-scale datasets [35]. A typical misclassification involves assigning an image having multiple concepts to a closely related class. An instance of such misclassification is depicted in Figure 3, where identical classes may be represented across different nodes. To avoid instances with the same meaning be regarded as negative samples, we introduce a node-wise taxonomy.

**Taxonomic Node.** In the conceptualization of our benchmark, we utilize a hierarchical semantic taxonomy. A taxonomic node assigns each direct child as one cluster. One cluster consists of all images belonging to the child and its descents. Figure 1 ① graphically illustrates the hierarchical structure of a synset. Notably, the node level indicates the depth within the hierarchical structure; hence, a node positioned at a lower level represents a more abstract, high-level concept.

## 4.2. Discriminative Discernment

This part details our empirical study on the overlap and aSTD across all nodes within the IN20K dataset for six distinct SSL models and one supervised model (DeiT). In the lower-level nodes of the taxonomy, where classes are diverse, distinguishing between them takes few effort. As we ascend to higher-level nodes, the granularity becomes increasingly fine-grained. The results, as summarized in Table 1, highlight the effectiveness of SSL methods in semantic learning. It is observed that SD models (DINO and iBOT) surpass other SSL models and exhibit competitive performance with supervised models (DeiT), particularly within the coarse semantic levels (levels 1-9). MIM demonstrates limited effectiveness, accompanied by a notable variance. In summation, while a discernible disparity exists between SSL and supervised models, it is not pronounced and predominantly resides within the domain of fine-grained classification.

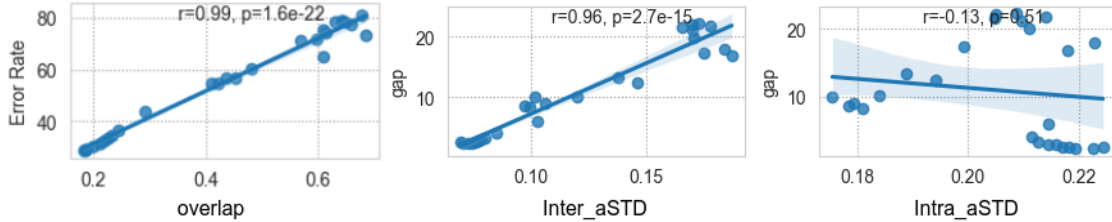


Figure 2. Overlap signifies separability and aSTD denotes consistency. “error rate” represents the performance on IN1K using  $k=10$  for KNN. “gap” refers to the accuracy differential between linear probing and KNN. “r” and “p” denote Pearson product-moment correlation coefficient and the p-value associated for the two-sided hypothesis test, respectively.

Table 1. Comparative analysis of overlap and aSTD for SSL models and DeiT on 16K synsets grouped by node levels. ‘AVG’ denotes the average metrics across all nodes. MIM shows limited effectiveness in learning semantic representations. SD methods are much effective in extracting coarse semantics for low levels (1-9).

level	overlap ↓							aSTD ↓						
	MAE	MoCo	SiT	MSN	DINO	iBOT	DeiT	MAE	MoCo	SiT	MSN	DINO	iBOT	DeiT
1	0.753	0.696	<b>0.661</b>	0.72	0.672	0.7	0.747	0.12	0.059	0.071	0.048	0.058	0.053	<b>0.045</b>
2	0.599	0.516	0.497	0.534	<b>0.493</b>	0.519	0.55	0.124	0.072	0.081	0.066	0.07	0.067	<b>0.062</b>
3	0.663	0.54	0.54	0.551	<b>0.521</b>	0.525	0.539	0.135	0.088	0.096	0.086	0.085	0.081	<b>0.077</b>
4	0.71	0.643	0.645	0.644	<b>0.629</b>	<b>0.629</b>	0.652	0.148	0.104	0.116	0.087	0.101	0.095	<b>0.081</b>
5	0.707	0.624	0.636	0.621	0.607	<b>0.606</b>	0.624	0.147	0.105	0.115	0.093	0.101	0.097	<b>0.085</b>
6	0.707	0.61	0.619	0.609	<b>0.592</b>	0.593	0.61	0.146	0.106	0.117	0.099	0.103	0.099	<b>0.091</b>
7	0.742	0.624	0.642	0.614	0.603	<b>0.6</b>	<b>0.6</b>	0.147	0.107	0.118	0.107	0.103	0.101	<b>0.099</b>
8	0.738	0.618	0.638	0.602	0.594	0.59	<b>0.588</b>	0.151	0.114	0.124	0.122	0.111	0.11	<b>0.108</b>
9	0.773	0.668	0.684	0.652	0.644	<b>0.642</b>	0.644	0.16	0.124	0.132	0.128	0.118	0.119	<b>0.119</b>
10	0.79	0.702	0.713	0.686	0.677	0.677	<b>0.675</b>	0.166	0.13	0.137	0.139	0.124	0.125	<b>0.128</b>
11	0.83	0.74	0.742	0.718	0.713	0.712	<b>0.706</b>	0.168	0.138	0.146	0.154	0.128	0.132	<b>0.136</b>
12	0.843	0.748	0.746	0.722	0.721	0.724	<b>0.713</b>	0.165	0.143	0.154	0.173	0.134	0.137	<b>0.138</b>
13	0.867	0.762	0.756	0.729	0.732	0.727	<b>0.718</b>	0.163	0.146	0.156	0.192	0.134	0.14	<b>0.143</b>
14	0.838	0.727	0.741	0.709	0.714	0.707	<b>0.691</b>	0.163	0.154	0.178	0.19	0.136	0.145	<b>0.138</b>
15	0.82	0.713	0.724	0.696	0.69	0.69	<b>0.668</b>	0.159	0.149	0.188	0.213	0.14	0.144	<b>0.14</b>
16	0.84	0.751	0.755	0.722	0.728	0.721	<b>0.677</b>	0.154	0.15	0.184	0.229	0.144	0.148	<b>0.135</b>
17	0.865	0.79	0.775	0.772	0.759	0.772	<b>0.791</b>	0.17	0.162	0.209	0.224	0.144	0.155	<b>0.13</b>
AVG	0.771	0.674	0.678	0.661	<b>0.651</b>	0.652	0.653	0.154	0.125	0.141	0.144	0.117	0.118	<b>0.113</b>

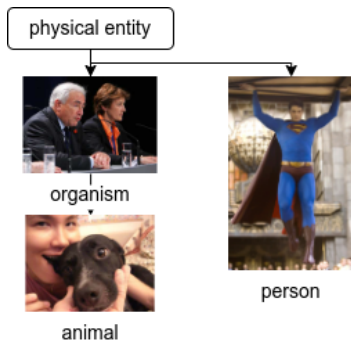


Figure 3. Example of inconsistent tagging in IN21K. Human can be found in different nodes, e.g., organism, animal, and person.

### 4.3. Generalizability

We elucidate the generalization capabilities of models on downstream tasks through two illustrative scenarios. These scenarios enable the prediction of model performance on distance-based tasks, such as image retrieval and K-Nearest Neighbors (KNN), by examining the overlap on relevant nodes on our benchmark.

**Buildings.** Oxford & Paris [33] are benchmarks commonly utilized for the assessment of image retrieval algorithms. To forecast model performance, we identify corresponding nodes via a closely related synset in WordNet, specifically “building.n.01”. Within this node, we discover 237 children clusters related to the “building.n.01” node and compute its overlap. Then, we compare mean Average Precision (mAP) [32] for the Medium set [33] with the over-

Table 2. Comparison between Image retrieval performance (mAP) for Medium on Oxford & Paris and overlap on synset “building.n.01”. The overlap of “building.n.01” ranks well the performance on Oxford & Paris.

	mAP $\uparrow$		overlap $\downarrow$
	roxford5k	rparis6k	building.n.01
DINO	0.3503 (3)	0.6120 (2)	0.5486 (2)
MAE	0.1072 (6)	0.2589 (6)	0.6962 (6)
MSN	<b>0.3590 (1)</b>	0.5749 (3)	0.5678 (4)
MoCo	0.2909 (4)	0.5457 (4)	0.5618 (3)
SiT	0.2444 (5)	0.4907 (5)	0.5922 (5)
iBOT	0.3562 (2)	<b>0.6313 (1)</b>	<b>0.5466 (1)</b>

lap among these 237 clusters, as presented in Table 2. Despite the differences between Oxford & Paris and “building.n.01” (see comparison in Appendix 8.2), the degree of overlap within the “building.n.01” synset serves as a predictive measure for image retrieval performance on the Oxford and Paris datasets. The empirical data suggests that models with lower overlap values tend to exhibit enhanced mAP scores.

**Pets and Flowers.** We delve into the capability of models to differentiate between highly similar classes – discriminative discernment. Notably, the Pets [31] and Flowers [40] datasets serve as the benchmarks for this evaluation, with detailed information accessible in Appendix 8.2. As delineated in Table 3, a comparative analysis of KNN accuracy and overlap across related synsets demonstrates that overlap is an efficacious indicator of model performance on these nuanced tasks. The overlap of a synset indicates the performance of its related downstream tasks.

Table 3. Comparison between KNN (k=10) performance (accuracy) on Pets and Flowers and overlap on synsets “cat.n.01”, “dog.n.01”, and “flower.n.01”. Given a synset, the lower overlap between its clusters the higher performance of its related downstream tasks will be.

	ACC $\uparrow$	overlap $\downarrow$		ACC $\uparrow$	overlap $\downarrow$
	Pets	cat.n.01	dog.n.01	Flowers	flower.n.01
DINO	<b>90.11</b>	<b>0.6648</b>	<b>0.4946</b>	<b>89.36</b>	<b>0.5894</b>
MAE	46.96	0.8927	0.8803	59.83	0.7457
MSN	89.83	0.6569	0.4624	81.61	0.6017
MoCo	84.76	0.6818	0.5453	82.34	0.6285
SiT	83.83	0.7406	0.6058	83.81	0.6290
iBOT	88.91	0.6723	0.463	87.56	0.5837

## 5. Findings

**Detrimental Potential of Supervised Learning.** While supervised learning can ostensibly enhance the acquisition

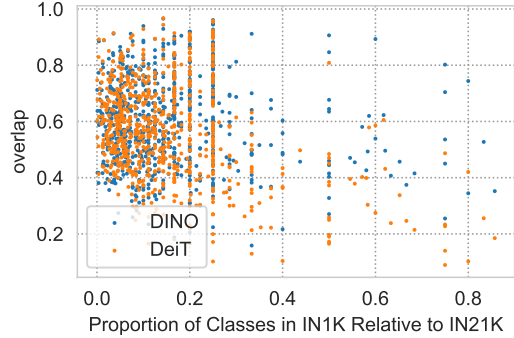


Figure 4. Relationship between class ratio (IN1K vs. IN21K) and overlap for DINO and DeiT. DeiT demonstrates the trend of increased supervision leading to reduced overlap.

of semantic representations, its success highly depends on the effectiveness of labels. As Table 4 delineates, the representations of DeiT can be transferred to Pets, yet fail to Flowers. We observe that there are a small portion of classes related to flowers in IN1K, indicating a limited present of certain classes leads to a skewed knowledge base. Consequently, supervised models suffer from transferring knowledge to a problem with domain shift. Figure 4 corroborates this assertion, illustrating the interplay between dataset divergence and class overlap, where X-axis denotes the ratio of the number of classes in IN1K to the number of classes in IN21K for a given synset, Y-axis denotes the respective overlap. Each data points elucidates the degree of separability amidst dataset shift. Contrastingly, DINO maintains a consistent mean overlap irrespective of the dataset disparity, suggesting an immunity to domain shift. DeiT, however, excels in the presence of small dataset shift (high ratio) but struggles to distinguish between unencountered synsets.

*\$ Is it feasible to retain discriminability amidst supervision?*

Table 4. KNN performance on IN1K does not adequately translate to classify Flowers. Herein, we report KNN precision (k=10) for IN1K, Flowers; the overlap for synsets “flower.n.01” and pet (“cat.n.01” and “dog.n.01”), respectively.

	IN1K	Flowers	flower.n.01	Pets	pet
DeiT	80.82	72.69	0.6171	91.58	0.5141
DINO	76.18	89.36	0.5894	90.11	0.5804

**Class Bias of Self-supervised Learning.** While the class categories within the training dataset are agnostic to SSL models, these models manifest either a propensity or difficulty in internalizing semantic representations from specific class categories. To probe this phenomenon, we assessed the class overlap for each model. The resulting histograms, as depicted in Figure 5, elucidate a notable pattern: SSL

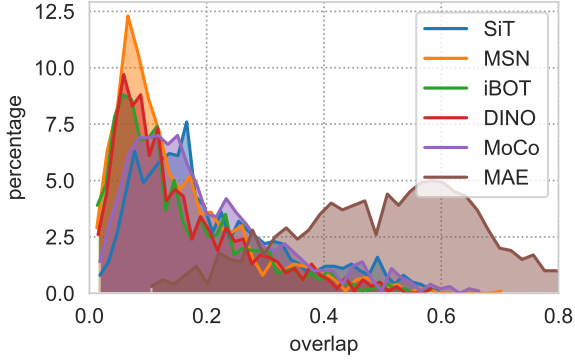


Figure 5. Histogram of overlaps from 1K classes on IN1K for SSL models. Classes that are considered ‘easy’ display lower overlap, while ‘hard’ classes exhibit higher overlap. Though SSL methods are agnostic to the labels, these classes are not learned equally.

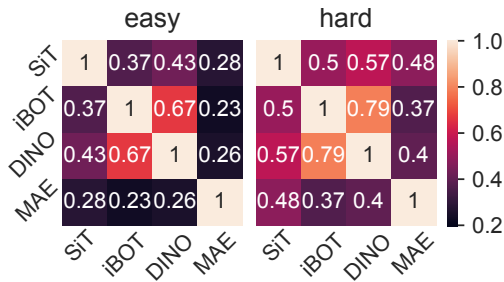


Figure 6. Jaccard similarity coefficient between 100 easy classes (left) and between 100 hard classes (right). The coefficient for random 100 classes is 0.1. SSL models show agreements with

models do not uniformly learn the semantic factors from samples for the classes in the training set. In light of this observation, we meticulously compiled two distinct subsets of 100 classes from IN1K for each model; one subset encompassed the ‘easy’ classes characterized by the lowest overlap metrics, while the other comprised the ‘hard’ classes, distinguished by the highest overlap metrics. Subsequently, we applied the Jaccard similarity coefficient to quantify the similarity between two subsets by counting the proportion of shared class commonality. Under the hypothesis of randomness, two arbitrary selections of 100 classes from IN1K would yield a Jaccard coefficient of approximately 0.1. Contrary to this baseline, as delineated in Figure 6, a pronounced commonality within two subsets was observed among the SSL models. Notably, MAE demonstrates a lower concordance with other SSL models for the ‘easy’ subset, whereas DINO and iBOT exhibit parallel behaviors for both two subsets. Especially within the ‘hard’ classes, all models indicate high commonality. Our investigative results cast light on the intrinsic difficulties of SSL models encounter when engaging with the ‘hard’ classes.

*§ Which intrinsic limitations within the ‘hard’ classes present obstacles to the learning process?*

## 6. Computational Cost

We run experiments on a machine with a single RTX 3060, i7-12700, and 32G memory to compare the speed of evaluation with KNN. For a fair comparison, we employ faiss [21], a library for efficient similarity search, to run KNN on a single GPU. Table 5 reports the runtime comparison of our protocol with KNN on IN1K for DINO. Each trial repeats 7 times. We can see that our protocol can significantly reduce the runtime by sampling a small proportion of the data without losing performance. The reported runtime excludes the feature extraction.

Table 5. Computational cost comparison with fast KNN on IN1K. Our evaluation can speed up 3.4x without losing performance and 3.9x faster than fast KNN.

	Statistical Metrics		
$n$	0.3	0.5	1
$t$ (s $\pm$ ms)	9.66 $\pm$ 77.2	16.3 $\pm$ 139	33.1s $\pm$ 234
overlap	0.1344	0.1344	0.1345
fast KNN			
$k$	1	10	20
$t$ (s $\pm$ ms)	38 $\pm$ 245	38.5 $\pm$ 255	39.1 $\pm$ 459
accuracy	0.7252	0.7490	0.7453

## 7. Conclusion

In this study, we introduce the Statistical Metric Learning Benchmark (SMLB) and devise two novel distance-based evaluation metrics – overlap and aSTD – to assess the efficacy of semantic representations beyond mere accuracy. Our comprehensive analysis of self-supervised learning (SSL) models, utilizing the SMLB, focuses on their discriminative discernment and generalizability. To the best of our knowledge, SMLB is the first large-scale benchmark that integrates both the diversity and granularity of class categorizations. The key insights garnered from our investigation are threefold: firstly, SSL models demonstrate proficiency in capturing coarse semantic details; secondly, supervised learning approaches hinder the models’ ability to adapt to dataset shifts; and thirdly, the ‘hard’ classes intrinsically challenge the SSL process.

**Limitation & Future Work.** While our evaluation methodology is model-agnostic and adaptable to diverse architectures, our current analysis is confined to Vision Transformers (ViTs). Additionally, the 16K nodes within our benchmark encompass instances of mislabeling, a common issue in large-scale datasets. Future endeavors will explore the impact of different architectural choices and refine the evaluation nodes to enhance both efficiency and effectiveness in the evaluation of semantic representation learning.



## References

- [1] Mahmoud Assran, Mathilde Caron, Ishan Misra, Piotr Bojanowski, Florian Bordes, Pascal Vincent, Armand Joulin, Mike Rabbat, and Nicolas Ballas. Masked siamese networks for label-efficient learning. In *Computer Vision—ECCV 2022: 17th European Conference, Tel Aviv, Israel, October 23–27, 2022, Proceedings, Part XXXI*, pages 456–473. Springer, 2022. 4
- [2] Sara Atito, Muhammad Awais, and Josef Kittler. SiT: Self-supervised vSion transformer. *ArXiv preprint*, abs/2104.03602, 2021. 1, 2, 4
- [3] Sara Atito, Muhammad Awais, and Josef Kittler. GMMML is all you need. *ArXiv preprint*, abs/2205.14986, 2022. 1, 2, 4
- [4] Mathilde Caron, Ishan Misra, Julien Mairal, Priya Goyal, Piotr Bojanowski, and Armand Joulin. Unsupervised learning of visual features by contrasting cluster assignments. In *Advances in Neural Information Processing Systems*, pages 9912–9924. Curran Associates, Inc., 2020. 2
- [5] Mathilde Caron, Hugo Touvron, Ishan Misra, Hervé Jégou, Julien Mairal, Piotr Bojanowski, and Armand Joulin. Emerging properties in self-supervised vision transformers. *ArXiv preprint*, abs/2104.14294, 2021. 2, 4
- [6] Binghui Chen, Weihong Deng, Biao Wang, and Lei Zhang. Confusion-based metric learning for regularizing zero-shot image retrieval and clustering. *IEEE Transactions on Neural Networks and Learning Systems*, pages 1–14, 2022. 2
- [7] Ting Chen, Simon Kornblith, Mohammad Norouzi, and Geoffrey E. Hinton. A simple framework for contrastive learning of visual representations. In *Proceedings of the 37th International Conference on Machine Learning, ICML 2020, 13–18 July 2020, Virtual Event*, pages 1597–1607. PMLR, 2020. 1, 2
- [8] Xinlei Chen, Saining Xie, and Kaiming He. An empirical study of training self-supervised vision transformers. *ArXiv preprint*, abs/2104.02057, 2021. 4
- [9] Simon Coghlan, Tim Miller, and Jeannie Paterson. Good proctor or “big brother”? ethics of online exam supervision technologies. 34(4):1581–1606, 2021. 2
- [10] Andong Deng, Taojiannan Yang, and Chen Chen. A large-scale study of spatiotemporal representation learning with a new benchmark on action recognition. *CoRR*, abs/2303.13505, 2023. 3
- [11] Jiankang Deng, Jia Guo, Niannan Xue, and Stefanos Zafeiriou. Arcface: Additive angular margin loss for deep face recognition. In *Proceedings of the IEEE/CVF conference on computer vision and pattern recognition*, pages 4690–4699, 2019. 2
- [12] Jacob Devlin, Ming-Wei Chang, Kenton Lee, and Kristina Toutanova. BERT: Pre-training of deep bidirectional transformers for language understanding. In *Proceedings of the 2019 Conference of the North American Chapter of the Association for Computational Linguistics: Human Language Technologies, Volume 1 (Long and Short Papers)*, pages 4171–4186, Minneapolis, Minnesota, 2019. Association for Computational Linguistics. 3
- [13] Carl Doersch, Abhinav Gupta, and Alexei A. Efros. Unsupervised visual representation learning by context prediction. In *2015 IEEE International Conference on Computer Vision (ICCV)*, pages 1422–1430. IEEE, 2015. 2, 11
- [14] Alaaeldin El-Nouby, Natalia Neverova, Ivan Laptev, and Hervé Jégou. Training vision transformers for image retrieval. *CoRR*, abs/2102.05644, 2021. 2
- [15] Christiane Fellbaum. *WordNet: An electronic lexical database*. MIT press, 1998. 2, 3, 5
- [16] Zheren Fu, Yan Li, Zhendong Mao, Quan Wang, and Yongdong Zhang. Deep metric learning with self-supervised ranking. In *Proceedings of the AAAI Conference on Artificial Intelligence*, pages 1370–1378, 2021. 2
- [17] Raia Hadsell, Sumit Chopra, and Yann LeCun. Dimensionality reduction by learning an invariant mapping. In *2006 IEEE Computer Society Conference on Computer Vision and Pattern Recognition (CVPR’06)*, pages 1735–1742. IEEE. 2
- [18] Kaiming He, Haoqi Fan, Yuxin Wu, Saining Xie, and Ross B. Girshick. Momentum contrast for unsupervised visual representation learning. In *2020 IEEE/CVF Conference on Computer Vision and Pattern Recognition, CVPR 2020, Seattle, WA, USA, June 13–19, 2020*, pages 9726–9735. IEEE, 2020. 4
- [19] Kaiming He, Xinlei Chen, Saining Xie, Yanghao Li, Piotr Dollar, and Ross Girshick. Masked autoencoders are scalable vision learners. In *2022 IEEE/CVF Conference on Computer Vision and Pattern Recognition (CVPR)*, pages 15979–15988. IEEE, 2022. 1, 4, 11, 13
- [20] Steven CH Hoi, Wei Liu, and Shih-Fu Chang. Semi-supervised distance metric learning for collaborative image retrieval and clustering. *ACM Transactions on Multimedia Computing, Communications, and Applications (TOMM)*, 6(3):1–26, 2010. 2
- [21] Jeff Johnson, Matthijs Douze, and Hervé Jégou. Billion-scale similarity search with GPUs. *IEEE Transactions on Big Data*, 7(3):535–547, 2019. 8
- [22] Mahmut Kaya and Hasan Şakir Bilge. Deep metric learning: A survey. 11(9):1066. 1
- [23] Syed Safwan Khalid, Muhammad Awais, Zhenhua Feng, Chi Ho Chan, Ammarah Farooq, Ali Akbari, and Josef Kittler. Npt-loss: Demystifying face recognition losses with nearest proxies triplet. *IEEE transactions on pattern analysis and machine intelligence*, 2022. 1, 2
- [24] Alexander Kolesnikov, Xiaohua Zhai, and Lucas Beyer. Revisiting self-supervised visual representation learning. In *2019 IEEE/CVF Conference on Computer Vision and Pattern Recognition (CVPR)*, pages 1920–1929. IEEE. 2
- [25] Weiyang Liu, Yandong Wen, Zhiding Yu, and Meng Yang. Large-margin softmax loss for convolutional neural networks. In *Proceedings of the 33rd International Conference on Machine Learning, ICML 2016, New York City, NY, USA, June 19–24, 2016*, pages 507–516. JMLR.org, 2016. 2
- [26] Shentong Mo, Zhun Sun, and Chao Li. Siamese prototypical contrastive learning. In *Proceedings of British Machine Vision Conference*, 2021. 1
- [27] Shentong Mo, Zhun Sun, and Chao Li. Rethinking prototypical contrastive learning through alignment, uniformity and correlation. In *Proceedings of British Machine Vision Conference*, 2022. 2

- [28] Shentong Mo, Zhun Sun, and Chao Li. Representation disentanglement in generative models with contrastive learning. In *2023 IEEE/CVF Winter Conference on Applications of Computer Vision (WACV)*, pages 1531–1540, 2023. [2](#)
- [29] Kevin Musgrave, Serge J. Belongie, and Ser-Nam Lim. A metric learning reality check. In *Computer Vision - ECCV 2020 - 16th European Conference, Glasgow, UK, August 23-28, 2020, Proceedings, Part XXV*, pages 681–699. Springer, 2020. [2](#), [3](#)
- [30] Maxime Oquab, Timothée Darcet, Theo Moutakanni, Huy V. Vo, Marc Szafraniec, Vasil Khalidov, Pierre Fernandez, Daniel Haziza, Francisco Massa, Alaaeldin El-Nouby, Russell Howes, Po-Yao Huang, Hu Xu, Vasu Sharma, Shang-Wen Li, Wojciech Galuba, Mike Rabbat, Mido Assran, Nicolas Ballas, Gabriel Synnaeve, Ishan Misra, Herve Jegou, Julien Mairal, Patrick Labatut, Armand Joulin, and Piotr Bojanowski. DINOv2: Learning robust visual features without supervision, 2023. [1](#)
- [31] Omkar M Parkhi, Andrea Vedaldi, Andrew Zisserman, and CV Jawahar. Cats and dogs. In *2012 IEEE conference on computer vision and pattern recognition*, pages 3498–3505. IEEE, 2012. [2](#), [7](#), [11](#)
- [32] James Philbin, Ondrej Chum, Michael Isard, Josef Sivic, and Andrew Zisserman. Object retrieval with large vocabularies and fast spatial matching. In *2007 IEEE conference on computer vision and pattern recognition*, pages 1–8. IEEE, 2007. [6](#)
- [33] Filip Radenovic, Ahmet Iscen, Giorgos Tolias, Yannis Avrithis, and Ondrej Chum. Revisiting oxford and paris: Large-scale image retrieval benchmarking. In *2018 IEEE Conference on Computer Vision and Pattern Recognition, CVPR 2018, Salt Lake City, UT, USA, June 18-22, 2018*, pages 5706–5715. Computer Vision Foundation / IEEE Computer Society, 2018. [2](#), [3](#), [6](#)
- [34] Ankit Singh Rawat, Aditya K Menon, Wittawat Jitkrittum, Sadeep Jayasumana, Felix Yu, Sashank Reddi, and Sanjiv Kumar. Disentangling sampling and labeling bias for learning in large-output spaces. In *International Conference on Machine Learning*, pages 8890–8901. PMLR, 2021. [2](#)
- [35] Tal Ridnik, Emanuel Ben Baruch, Asaf Noy, and Lihi Zelnik. Imagenet-21k pretraining for the masses. In *Proceedings of the Neural Information Processing Systems Track on Datasets and Benchmarks 1, NeurIPS Datasets and Benchmarks 2021, December 2021, virtual*, 2021. [5](#)
- [36] Oren Rippel, Manohar Paluri, Piotr Dollár, and Lubomir D. Bourdev. Metric learning with adaptive density discrimination. In *4th International Conference on Learning Representations, ICLR 2016, San Juan, Puerto Rico, May 2-4, 2016, Conference Track Proceedings*, 2016. [3](#)
- [37] Olga Russakovsky, Jia Deng, Hao Su, Jonathan Krause, Sanjeev Satheesh, Sean Ma, Zhiheng Huang, Andrej Karpathy, Aditya Khosla, Michael Bernstein, et al. Imagenet large scale visual recognition challenge. *International journal of computer vision*, 115:211–252, 2015. [2](#), [3](#), [5](#), [11](#)
- [38] Florian Schroff, Dmitry Kalenichenko, and James Philbin. FaceNet: A unified embedding for face recognition and clustering. In *Proceedings of the IEEE conference on computer vision and pattern recognition*, pages 815–823. [2](#)
- [39] Zhiqing Sun, Yikang Shen, Qinhong Zhou, Hongxin Zhang, Zhenfang Chen, David Cox, Yiming Yang, and Chuang Gan. Principle-driven self-alignment of language models from scratch with minimal human supervision. *arXiv preprint arXiv:2305.03047*, 2023. [2](#)
- [40] K Tung. Flowers Dataset, 2020. [7](#)
- [41] Aishwarya Venkataramanan, Martin Laviale, Cécile Figus, Philippe Usseglio-Polatera, and Cédric Pradalier. Tackling inter-class similarity and intra-class variance for microscopic image-based classification. In *Computer Vision Systems*, pages 93–103. Springer International Publishing. [3](#)
- [42] Fei Wang and Jimeng Sun. Survey on distance metric learning and dimensionality reduction in data mining. *Data mining and knowledge discovery*, 29(2):534–564, 2015. [1](#)
- [43] Jimpeng Wang, Ziyun Zeng, Bin Chen, Tao Dai, and Shu-Tao Xia. Contrastive quantization with code memory for unsupervised image retrieval. *Proceedings of the AAAI Conference on Artificial Intelligence*, 36(3):2468–2476, 2022. [2](#)
- [44] Shulei Wang. Self-supervised metric learning in multi-view data: A downstream task perspective. *Journal of the American Statistical Association*, pages 1–14, 2022. [2](#), [3](#)
- [45] Jiantao Wu and Shentong Mo. Object-wise masked autoencoders for fast pre-training. *arXiv preprint arXiv:2205.14338*, 2022. [1](#)
- [46] Jiantao Wu, Shentong Mo, Muhammad Awais, Sara Atito, Zhenhua Feng, and Josef Kittler. Masked momentum contrastive learning for zero-shot semantic understanding. *arXiv preprint arXiv:2308.11448*, 2023. [1](#)
- [47] Liu Yang and Rong Jin. Distance metric learning: A comprehensive survey. *Michigan State University*, 2(2):4, 2006. [1](#)
- [48] Dong Yi, Zhen Lei, Shengcai Liao, and Stan Z. Li. Learning face representation from scratch. *CoRR*, abs/1411.7923, 2014. [2](#)
- [49] Xiaohua Zhai, Joan Puigcerver, Alexander Kolesnikov, Pierre Ruysen, Carlos Riquelme, Mario Lucic, Josip Djolonga, Andre Susano Pinto, Maxim Neumann, Alexey Dosovitskiy, Lucas Beyer, Olivier Bachem, Michael Tschannen, Marcin Michalski, Olivier Bousquet, Sylvain Gelly, and Neil Houlsby. A large-scale study of representation learning with the visual task adaptation benchmark. [13](#)
- [50] Jinghao Zhou, Chen Wei, Huiyu Wang, Wei Shen, Cihang Xie, Alan Yuille, and Tao Kong. iBOT: Image BERT pre-training with online tokenizer. *ArXiv preprint*, abs/2111.07832, 2021. [4](#), [13](#)

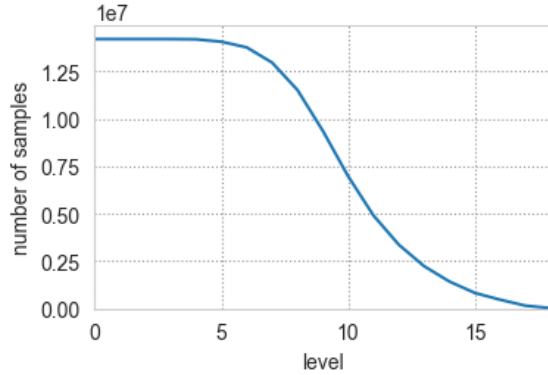


Figure 7. The numbers of classes and samples for each level.

## 8. Dataset

### 8.1. IN21K details

According to the distance to the root node, we assign a level for each node. The node level denotes the depth of the node in the semantic tree. The numbers of classes and samples are shown in Figure 7. A detailed summary of each level is in Table 6. On the top of the semantic tree, each cluster represents a coarse class consisting of diverse categories. Therefore, the node has more shared features and closer semantic concepts as it increases the level.

### 8.2. Dataset Comparison

**Oxford & Paris.** The Oxford Building dataset consists of 5,062 images from 11 different landmarks, and Paris dataset contains 6,412 images from Paris landmarks. In IN21K, the closest synset is “building.n.01” (“landmark” does not exist in IN21K). There are 236 children with 194,038 images for “building.n.01” from levels 7 to 11. Among them, there are 47 direct children. Figure 10 shows samples from Oxford & Paris as well as the “building.n.01” node. Therefore, the “building.n.01” node has far more diversity than Oxford&Paris. Despite the large disp\* between the node and the target datasets, our benchmark can still indicate the performance and show generalizability well.

**Dog&Cat.** The Pets dataset [31] has 12 cat breeds with 2,371 images and 25 dog breeds with 4,978 images. It is notable that there are lots of differences in breeds between Pets [31] and “cat.n.01” “dog.n.01” [37]. The samples from IN21K contain more irrelative elements, like humans. The categories of breeds in the two sets are also quite different.

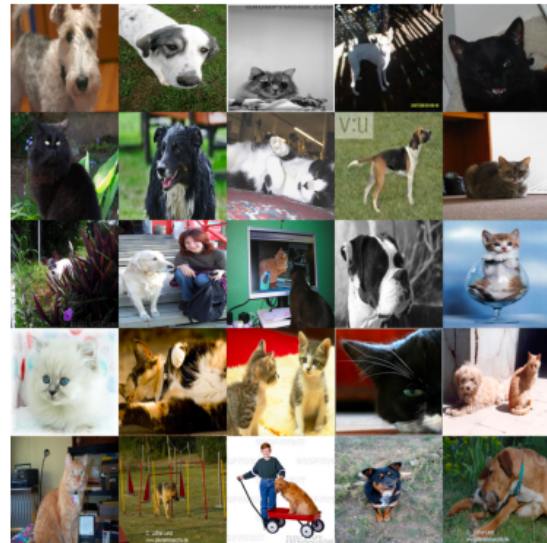
## 9. Evaluation Analysis

### 9.1. How important the normalization is?

Adding BatchNorm without affine transformation after ViT has been proven a helpful trick to improve downstream



Pets



cat.n.01 and dog.n.01

Figure 8. Sample comparison between Pets and the synsets related to dogs and cats in IN21K.

tasks [13, 19]. Our observations affirm that the normalization strategy reduces the domain shift. We compared three distinct normalization approaches to ascertain their impact on mitigating domain shift: 1) omission of normalization, 2) application of normalization using the mean and standard deviation of the target dataset, and 3) utilization of the mean and standard deviation from the source dataset. The comparative analysis of overlap for three normalization strategies, as detailed in Table 7, demonstrates that normalizing features using the mean and standard deviation derived from the target dataset yields superior performance across

Table 6. Brief summary of IN21K for each level.

level	classes	samples	children	leaf	Examples
0	21841	14197087	2	4	entity, sun, genet, munro, stoker
1	21837	14195721	11	0	physical entity, abstraction
2	21837	14195721	53	0	object, causal agent, matter, psychological feature, thing
3	21837	14195721	374	6	whole, person, substance, event, agent
4	21826	14183895	884	149	living thing, food, artifact, act, infectious agent
5	21595	14058407	1849	459	organism, cell, propulsion, action, activity
6	20971	13757813	2669	1124	benthos, heterotroph, animal, plant, jump
7	19523	12958083	3250	1799	hop, check-in, sport, motion
8	17161	11515127	3592	2320	riding, funambulism, rise, contact sport, outdoor sport
9	14099	9369930	3413	2722	equestrian sport, climb, acrobatics, track, jumping
10	10639	6972298	2515	2711	dressage, rock climbing, broad jump, high jump, bathe
11	7313	4906765	1799	2040	curvet, piaffe, fosbury flop, dead-man’s float, belly flop
12	4829	3367395	1138	1465	ball, professional baseball, hardball, perfect game, no-hit game
13	3046	2235397	802	902	wolf, dog, bear cub, soft-finned fish, spiny-finned fish
14	1915	1426986	483	664	wolf pup, puppy, ostariophysi, cypriniform fish, percoid fish
15	1115	828458	416	370	loach, cyprinid, sunfish, electric eel, catostomid
16	636	470730	188	344	carp, freshwater bream, tench, dace, chub
17	225	157373	37	173	domestic carp, european bream, common shiner, buffalo fish, hog sucker
18	37	26490	0	37	leather carp, mirror carp, black buffalo, toy manchester, sealyham terrier

Table 7. Overlaps on Pets with three normalization strategies: 1) no normalization 2) normalizing with the mean and std from the “target” dataset and 3) the “source” dataset. MoCo, MAE, and MSN highly rely on normalization.

Feature Normalization	None	Target	Source
DINO	0.1793	0.1544	0.1719
MAE	0.9410	0.7199	0.7447
MSN	1.0000	<b>0.1259</b>	<b>0.1375</b>
MoCo	0.2700	0.1955	0.2252
iBOT	<b>0.1793</b>	0.1402	0.1552

all models. The experimental results suggest that such normalization is effective in domain shift reduction.

## 9.2. Benchmark for Maximal Overlap

In previous experiments, we consider the average overlap of one cluster to other clusters. It reveals an overall distance distribution among clusters. It is notable that in the worst case, the overlap between the two most far away clusters is also one of the important criteria for distance metric. Therefore, we further analyze the maximal overlap for each node in Table 8. There is a similar trend with the average overlap that SSL models perform better on coarse semantic nodes.

## 9.3. Object-wise Similarity.

In this part, we extend our evaluation of local features to study their separability and consistency. Similarly, to study

Table 8. Comparative analysis of maximal overlap for SSL models and DeiT on 16K synsets grouped by node levels. ‘AVG’ denotes the average metrics across all nodes. DeiT surpasses others from levels 7-16.

	MAE	MoCo	SiT	MSN	DINO	iBOT	DeiT
1	0.942	0.909	0.923	0.917	<b>0.896</b>	0.9	0.94
2	0.849	0.786	0.764	<b>0.756</b>	0.774	0.789	0.789
3	0.868	0.786	0.792	0.819	0.78	0.781	<b>0.779</b>
4	0.904	0.862	0.866	0.857	<b>0.85</b>	0.854	0.862
5	0.898	0.85	0.857	0.845	0.839	<b>0.838</b>	0.844
6	0.88	0.824	0.833	0.825	<b>0.815</b>	<b>0.815</b>	0.823
7	0.898	0.83	0.839	0.816	0.814	0.815	<b>0.809</b>
8	0.885	0.813	0.825	0.801	0.797	0.794	<b>0.79</b>
9	0.905	0.847	0.857	0.833	0.831	0.83	<b>0.828</b>
10	0.918	0.873	0.878	0.861	0.859	0.858	<b>0.854</b>
11	0.936	0.881	0.881	0.868	0.866	0.865	<b>0.862</b>
12	0.937	0.883	0.878	0.868	0.867	0.868	<b>0.865</b>
13	0.944	0.886	0.883	0.869	0.874	0.867	<b>0.859</b>
14	0.946	0.888	0.895	0.866	0.877	0.875	<b>0.858</b>
15	0.926	0.861	0.87	0.854	0.846	0.845	<b>0.834</b>
16	0.927	0.884	0.887	0.853	0.866	0.868	<b>0.807</b>
17	0.973	0.932	0.93	0.94	<b>0.93</b>	0.934	0.934
AVG	0.914	0.859	0.862	0.85	0.846	0.847	0.843

the local features within an image  $x$ , we define the *intra-object* pair as the pair of image patches from the same object, and *inter-object* pair as the pair of image patches from

Table 9. Object-wise statistical measurement on ImageNet-S 919 subset. “fn\_type” denotes feature normalization type of the direction of normalization: 0 for the samples, 1 for the patches within an image, 2 for both.

fn_type	aSTD			overlap		
	0	1	2	0	1	2
MAE	<b>0.060</b>	0.088	0.087	0.630	0.763	<b>0.576</b>
iBOT	<b>0.074</b>	0.117	0.116	0.649	0.737	<b>0.604</b>

different objects. For a given set of image patches  $x_p$  and their corresponding masks  $m_p$  that identify the object’s location, we can determine if patches originate from the same or different objects. Thus, we can define the intra- and inter-object similarity as:

$$\begin{aligned} s_{\text{OBJ}}^+(\mathbf{x}_i, \mathbf{x}_j) &= \text{sim}(\mathbf{z}_i, \mathbf{z}_j), \text{ if } \mathbf{m}_i = \mathbf{m}_j, \\ s_{\text{OBJ}}^-(\mathbf{x}_i, \mathbf{x}_j) &= \text{sim}(\mathbf{z}_i, \mathbf{z}_j), \text{ if } \mathbf{m}_i \neq \mathbf{m}_j. \end{aligned} \quad (5)$$

Our protocol provides a unified method for assessing the representations for both global and local semantics. For global semantics, we employ class labels to define positive pairs. In contrast, we utilize object segmentation to define positive pairs for local semantics. We collect the local features for each object over the whole dataset and compute the statistical metrics for two models: MAE [19] and iBOT [50]. We considered three normalization methods for the local features using the mean and std along the sample dimension (0), sequence dimension (1), and both (2). To compare the quality of dense features for SSL models, we conduct experiments on ImageNetS, a variant of ImageNet with semantic segmentation [49]. This dataset contains segmentation labels of the dominant object for images. 919 subset is the largest split with 12,419 images divided into 919 categories. Table 9 demonstrates overlap and aSTD on ImageNet-S 919 subset for MAE and iBOT with three normalization types. Though MAE has limited performance on global features, its local features have higher quality in indicating semantic distance than iBOT.

## 10. Efficiency

**Sampling.** Our proposed metrics are based on statistical distributions. Therefore, the quality of estimation is vital for the final result, which is affected by the number of samples. We study the estimation error of sampling a part of the samples in the data by comparing the metrics in the full dataset within a proportion of the dataset. The experiments are finished on a machine with a single RTX 3060, i7-12700, and 32G memory. Table 10 reports the spending time, KL, overlap, and aSTD for randomly picking  $n$  percent of samples. We can see that sampling 30% percent of data saves 91% evaluation time, maintaining similar results.

Table 10. Estimation error for  $n$  percent of the data.

$n$	time (s)	overlap	inter-aSTD	intra-aSTD
0.01	7.3486	0.1450	0.0553	0.2518
0.1	228.2575	0.1284	0.0554	0.2202
0.3	1010.3546	0.1261	0.0554	0.2179
0.5	2818.6852	0.1258	0.0554	0.2175
1.0	11161.6814	0.1255	0.0554	0.2171

**Runtime.** Our evaluation is effective in assessing representations on our large-scale benchmark. The whole evaluation process consists of two parts: feature extraction and computing overlaps. We evaluated each model on a machine with 4 RTX 2080 Ti GPUs, AMD EPYC 7502 (32 cores), and 256G memory. The runtime for feature extraction using 4 GPUs is 11 hours. Then, we compute the overlaps using 4 GPUs is 11 hours. Figure 9 shows the runtime of each node and its number of samples. The total computation time is 14,747 seconds.

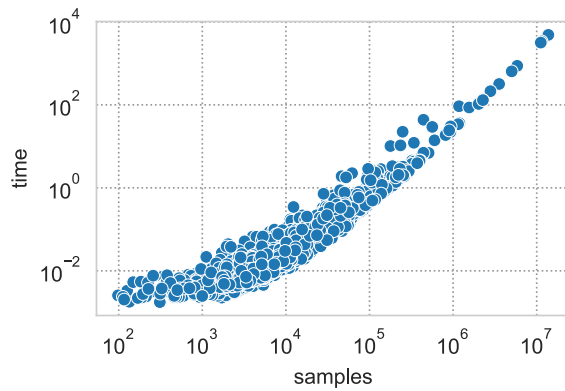


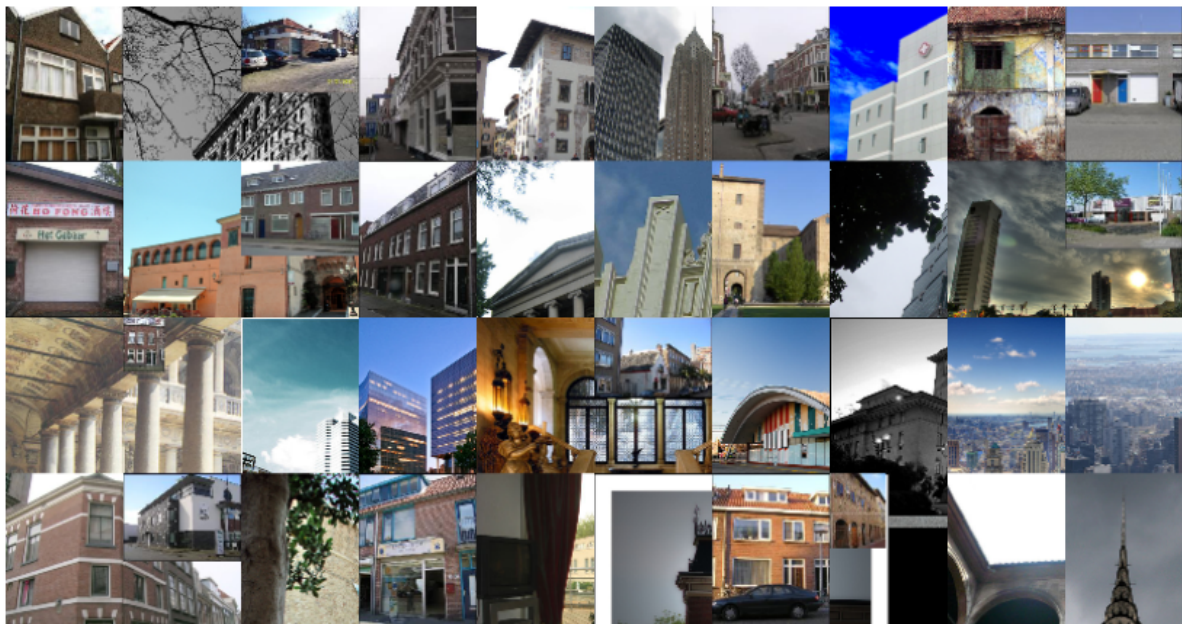
Figure 9. Computation cost of nodes. Each point demonstrates the evaluation time of a node without feature extraction and its sample number.



Paris



Oxford



building.n.01

Figure 10. Random samples from Oxford, Paris and “building.n.01”. One can see notable variability among these datasets: “building.n.01” exhibits a broad diversity of structures with minimal noise, like tourists.